Numerical study of the THM effects on the near-field safety of a hypothetical nuclear waste repository-BMT1 of the DECOVALEX III project. Part 2: Effects of THM coupling in continuous and homogeneous rocks

A. Millard, A. Rejeb, M. Chijimatsu, L. Jing, J. de Jonge, M. Kohlmeier, T.S. Nguyen, J. Rutqvist, M. Souley, Y. Sugita

Numerical study of the THM effects on the near-field safety of a hypothetical nuclear waste repository—BMT1 of the DECOVALEX III project. Part 2: Effects of THM coupling in continuous and homogeneous rocks

A. Millard (1), A. Rejeb (2), M. Chijimatsu (3), L. Jing (4), J. De Jonge (5), M. Kohlmeier (6), T.S. Nguyen (7), J. Rutqvist (8), M. Souley (9), and Y. Sugita (10)

(1) Commissariat a l'Energie Atomique (CEA), Paris, France
(2) Institut de Radioprotection et de Sûreté Nucléaire (IRSN), Paris, France
(3) Hazama Corporation, 2-5-5, Toranomon, Minato-ku, Tokyo 105-8479, Japan
(4) Royal Institute of Technology (KTH), Stockholm, Sweden
(5) University of Tuebingen, Tuebingen, Germany
(6) University of Hannover, Hannover, Germany
(7) Canadian Nuclear Safety Commission (CNSC), Ottawa, Canada
(8) Lawrence Berkeley National Laboratory (LBNL), Berkeley, USA
(9) INERIS-LAEGO, Ecole des Mines de Nancy, Nancy, France
(10) Japan Nuclear Cycle Development Institute (JNC), Ibaraki, Japan

Abstract

An evaluation of the importance of the thermo-hydro-mechanical couplings (THM) on the performance assessment of a deep underground radioactive waste repository has been made as a part of the international DECOVALEX III project. It is a numerical study that simulates a generic repository configuration in the near field in a continuous and homogeneous hard rock. A periodic repository configuration comprises a single vertical borehole, containing a canister surrounded by an over-pack and a bentonite layer, and the backfilled upper portion of the gallery. The thermo-hydro-mechanical evolution of the whole configuration is simulated over a period of 100 years. The importance of the rock mass's intrinsic permeability has been investigated through scoping calculations with three values: 10^{-17}, 10^{-18} and 10^{-19} m^2. Comparison of the results predicted by fully coupled THM analysis as well as partially coupled TH, TM and HM analyses, in terms of several predefined indicators of importance for performance assessment, enables us to identify the effects of the different combinations of couplings, which play a crucial role with respect to safety issues. The results demonstrate that temperature is hardly affected by the couplings. In contrast, the influence of the couplings on the mechanical stresses is considerable.

Keywords: Thermo-hydro-mechanical couplings; Performance assessment; Radioactive wastes

1. Introduction

The present paper is the second of three companion papers on bench mark test 1 (BMT1) of DECOVALEX III project [1]. The definition of the BMT1, as well as the model's conceptualization and characterization, are presented in the first companion paper [3]. This paper describes the works conducted during Phase B (BMT1B), which consists in scoping calculations for a hypothetical repository in continuous and homogeneous rock. The influence of some possible fractures will be further discussed in the third companion paper [4].

The definition of BMT1B is based on a hypothetical case of a Japanese conceptual repository design, located in a granitic formation at a depth of 1000 m [5]. The repository consists mainly of a series of parallel galleries, in which vertical depository boreholes are excavated with a central distance of 4.44 m. The depth of the depository hole is 4.13 m and its diameter is 2.22 m. The overpack (canister) for radioactive wastes would be emplaced at the top of the depository hole, and a bentonite buffer material would be compacted around the overpack. The details of the depository geometry design are given in Fig. 1. The tunnels would also be backfilled with a mixture of gravel and clay.

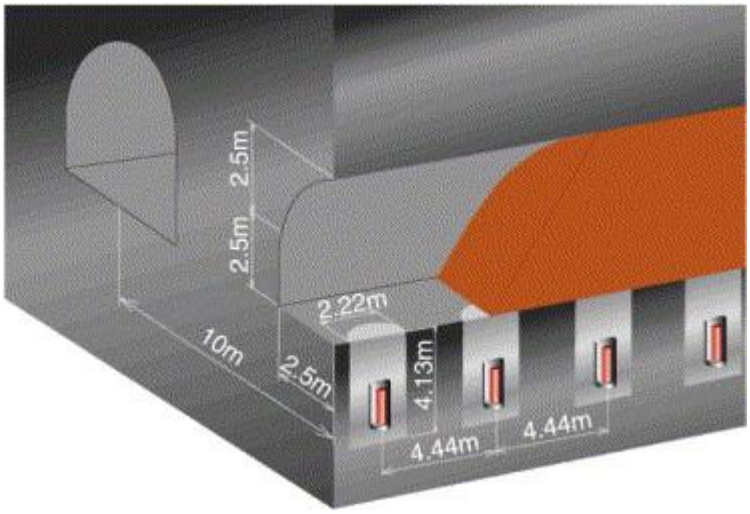

Fig. 1. Conceptual design of a hypothetical repository in Japan.

The bentonite considered as an engineered barrier in the hypothetical repository is the same as the one used in situ THM experiment at the Kamaishi mine. However, the permeability and strength characteristics of the rock mass are based on data obtained from sparsely fractured rock of the Canadian shield.

In order to evaluate the importance of the THM couplings on the repository performance assessment, performance measures characterizing the processes have been selected:

• evolution of the temperature in the buffer, and in particular the maximum temperature,

• evolution of the moisture content in the buffer, and in particular the time for full re-saturation,

• evolution of the stresses in the buffer and its maximum magnitudes,

• possibility of a rock-mass failure,

• maximum change of permeability in the rock mass.

2. Specification of the task

2.1. Geometry

In the task of BMT1B, the focus is placed on the near field and on a period during which the maximum temperature in the buffer is reached. Due to the assumed continuity and homogeneity of the rock mass, and the periodicity of the geometry of the galleries and the depository boreholes, the numerical simulations can be conducted on a repetitive web, as illustrated on Fig. 2. Moreover, the symmetry of the web itself makes it possible to consider only one quarter of the web for the calculations.

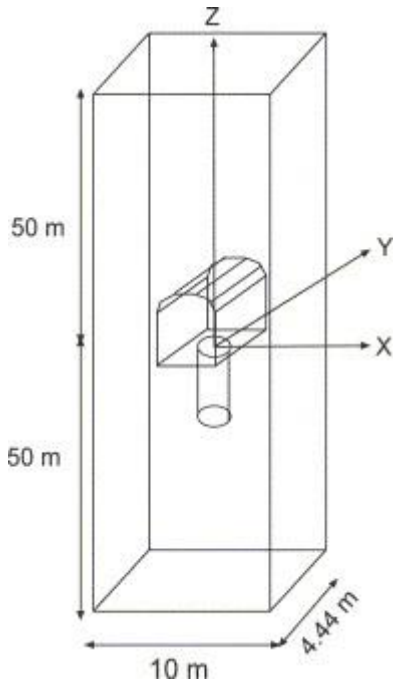

Fig. 2. Geometry of the repetitive web, considered in the analysis.

2.2. Initial and boundary conditions, modeling sequences

Prior to any excavation, the rock mass is supposed to be saturated and in equilibrium. The water pressure is equal to the hydrostatic pressure, which, at the depth of 1000 m, amounts to about 10 MPa. The temperature in the investigation domain is approximated by a uniform value of 45 °C, caused by the natural geothermal gradient. The vertical stress, due to the overburden load, is equal to σ_v = -25.6 MPa, and the horizontal stresses are equal to 1.5 σ_v.

From symmetry considerations, zero heat and mass fluxes, as well as zero normal displacements are prescribed on the lateral boundaries of the model. On the top and bottom boundaries, water pressure is set equal to the relevant hydrostatic pressure at their respective depths, and the initial temperature of 45 °C is maintained. The vertical displacements are prevented at the bottom, while the overburden load is maintained at the top of the model.

Starting from the in situ state of stresses, pressure and temperature, a first step consists in excavating the gallery and depository borehole. This leads to a transient state, before a new equilibrium is reached. Meanwhile, the temperature and pressure in the excavated openings

are set equal to 20 °C and 0 MPa, respectively. After a steady state is obtained, the overpack containing the canister, the buffer, and the backfill material are emplaced simultaneously, at an initial temperature of 20 °C, and different water contents, but free of stresses. From that instant, heat is released by the wastes, according to a decreasing law represented on Fig. 3. The response of the whole system is then studied over a 100-year's period, during which the thermal paroxysm is reached.

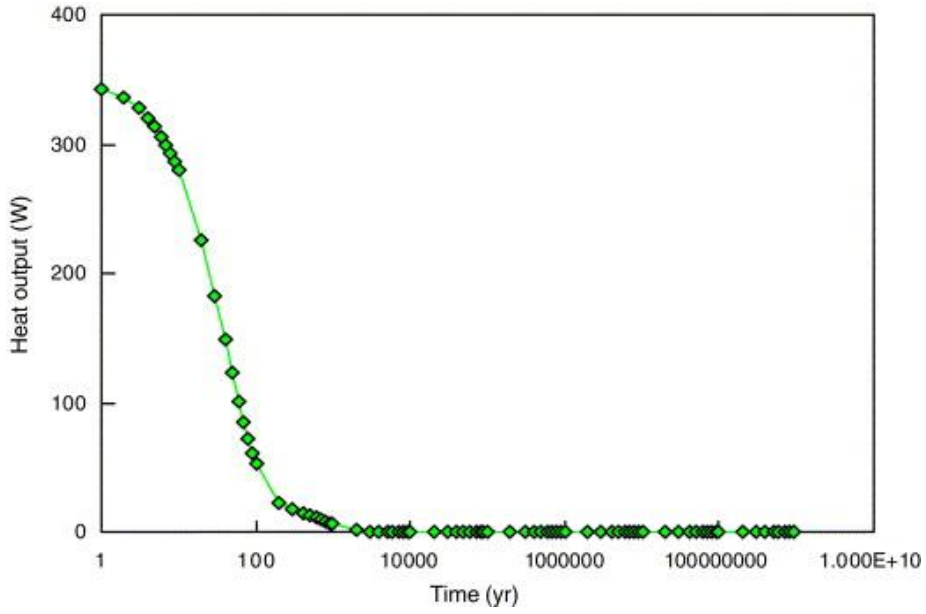

Fig. 3. Heat released by a waste canister.

The initial and boundary conditions of the different steps are summarized in Fig. 4.

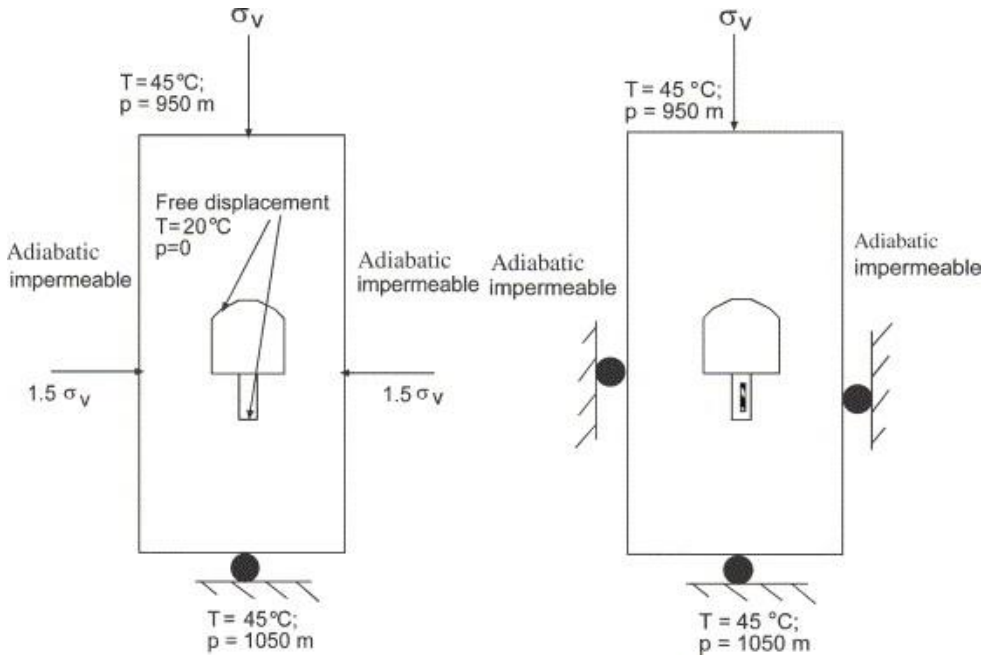

Fig. 4. Summary of initial and boundary conditions (left: before emplacement of wastes, right: after).

2.3. Material properties

The basic THM properties of the buffer material have been calibrated from laboratory tests, such as isothermal infiltration tests, swelling pressure test, and moisture flow under thermal gradient tests, during the project DECOVALEX II [2], [6] and [8] and against the results of an in situ heater test in Kamaishi Mine, as the phase A of the BMT1 project described in the companion paper [3].

The rock properties were also identified during phase A. However, because of the crucial role played by the rock-mass permeability on the resaturation of the buffer, it has been decided to consider three different values of the initial intrinsic permeability: 10^{-17}, 10^{-18} (which was considered as the base case) and 10^{-19} m^2. Moreover, a variation of the permeability with respect to either the porosity or the effective mean stress sM has been assumed:

$$K(\phi)=2.186\times10^{-10}\ \phi^3-5.185\times10^{-18}, \qquad (1)$$

$$K(\sigma_M) = 1.5 \times 10^{-15}\sigma_M^{-1.92} \text{ or}$$
$$K(\sigma_M) = 2.0 \times 10^{-18}\sigma_M^{-0.9}. \qquad (2)$$

Both are illustrated on Fig. 5. Most teams used the K(ϕ) relationship, based on data from the Canadian shield.

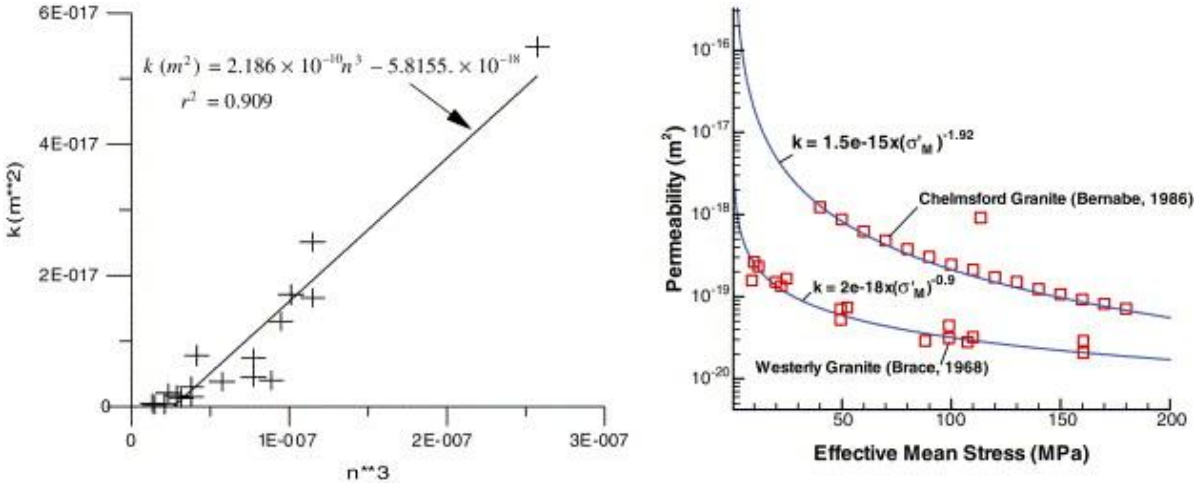

Fig. 5. Rock-mass intrinsic permeability functions.

The backfill is made of a mixture of bentonite (15%) and aggregates. Its swelling pressure was taken as proportional to the bentonite content.

All the parameters used by the different teams can be found in [9]. In Table 1 and Table 2, the properties which significantly differ from one team to another, and which may partly explain some differences in the results are summarized.

Table 1. Main different properties for the buffer

Team	Young's modulus (MPa)	Thermal expansion (°C)
CEA	150	3×10^{-5}
CNSC	150	3×10^{-6}
JNC	250	3×10^{-6}
SKI	26	3×10^{-5}
ISEB	100	8.21×10^{-6}

Table 2. Main different properties for the rock mass

Team	Permeability range (m2)	Biot's coefficient
CEA	10-17–10-19	1
CNSC	10-18–10-19	0.2
JNC	10-18–10-20	1
SKI	10-17–10-19	0.5

3. Finite element models and analysis

3.1. Numerical models

Five teams participated in the task BMT1B: CEA/IRSN (France), CNSC (Canada), ISEB/ISAG (Germany), JNC (Japan) and SKI/KTH (Sweden). All teams used fully coupled THM models. The detailed expressions of the models can be found in the companion paper [3] and in reference [7]. Their main features are recalled here:

• the gas pressure is supposed to be constant, equal to the atmospheric pressure,

• liquid water flow is governed by a generalized Darcy's law (or equivalent) where the conductivity depends on the saturation degree,

• vapor flow is induced by the thermal gradient, and, for SKI, by the pressure gradient,

• the bentonite swelling is accounted for either by a ‘Bishop-like’ effective stress or by a swelling stress function (JNC).

According to the periodic web geometry, all teams except JNC adopted a three-dimensional model. The JNC team used an axisymmetric model. The finite element codes used are listed in Table 3. Typical meshes are plotted on Fig. 6 and Fig. 7.

Table 3. Research team and simulation code

Research team	Code	Model type
CEA/IRSN	CASTEM 2000	3D
CNSC	FRACON	3D
JNC	THAMES	2D Axi
SKI	ROCMAS	3D
ISEB/ZAG	RF/RM	3D

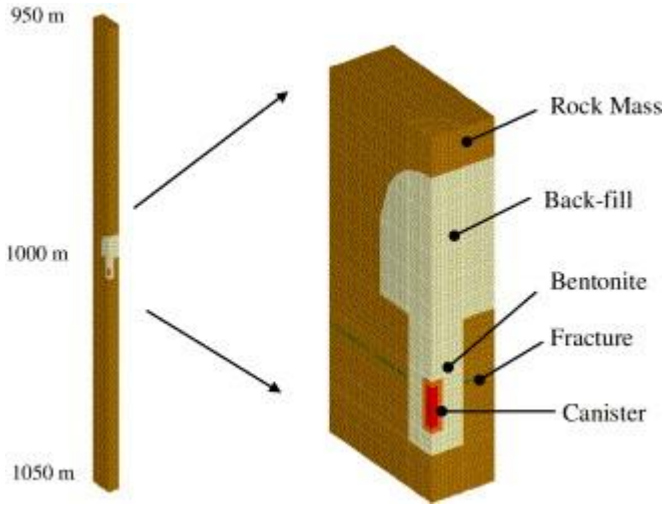

Fig. 6. Three-dimensionnal finite element model used by SKI/KTH.

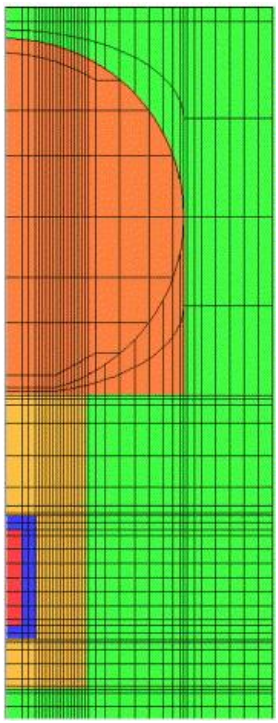

Fig. 7. Axisymmetric finite element model used by JNC: Zoom on the engineered bareer.

3.2. Coupled and partially coupled simulations

In order to investigate the influence of different combinations of couplings, the results of a fully coupled THM simulation are compared to partially coupled solutions: coupled TH/uncoupled M, coupled HM/uncoupled T, coupled TM/uncoupled H. In these simulations, the couplings are broken to one of the processes M, T or H, meaning that these processes are solved independent of the others. However, all simulations start with the same initial conditions, before the excavation of the rock, and after emplacement of the buffer and backfill. For all cases, the influence of the initial values of the rock-mass permeability has been investigated.

3.3. Analysis of rock-mass failure

From the calculated mechanical results, the stress history is post-processed in order to evaluate if some rock failure may occur. The integrity of the rock is estimated using the Hoek–Brown failure criterion, which can be written as [10]:

$$\sigma_1' = \sigma_3' + \sigma_{ci}\left(m_b \frac{\sigma_3'}{\sigma_{ci}} + s\right)^a, \qquad (3)$$

where σ'_1 and σ'_3 are, respectively, the maximum and minimum effective stresses at failure, m_b, s and a are constants which depend upon the characteristics of the rock mass and σ_{ci} is the uniaxial compressive strength of the intact rock. For the rock considered in the present case, regarded as a very good quality rock mass, the estimated values of these constants are as follows: a = 0.5, m_b = 17.5 and s = 0.19. and σ_{ci} = 123 MPa.

4. THM results

In this section, the results obtained by the different teams for the fully coupled THM analysis, are compared, and the influence of the rock-mass' initial permeability on the results is investigated as well. The results are evaluated on the basis of the performance measures defined in the introduction. In particular, some points of interest located in the buffer have been selected. They are shown in Fig. 8.

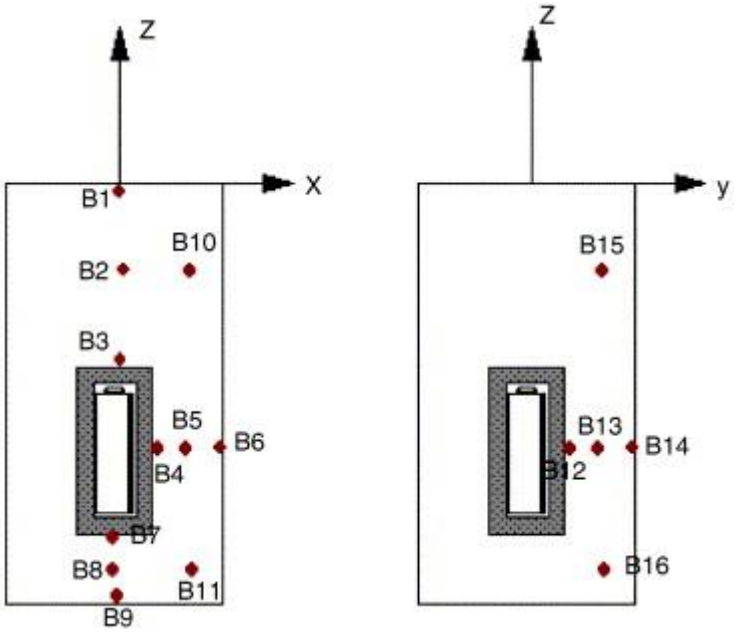

Fig. 8. Selected points of interest in the buffer.

4.1. THM results for the base case (K = 10^{-18} m^2)

4.1.1. Temperature evolution in the buffer and maximum temperature

Typical temperature profiles obtained at the various locations in the buffer are presented in Fig. 9. As could be expected, the maximum temperature is reached at the contact with the overpack, after about 35 years of heating. Three-dimensional models predict a value within the range of 75–80 °C, whereas the axisymmetric model (JNC) leads to a slightly higher temperature. According to SKI/KTH predictions, after 1000 years, the heat power is down to a few percents of its initial value, and the temperature has decreased to about 46 °C, one degree above the ambient temperature of 45 °C.

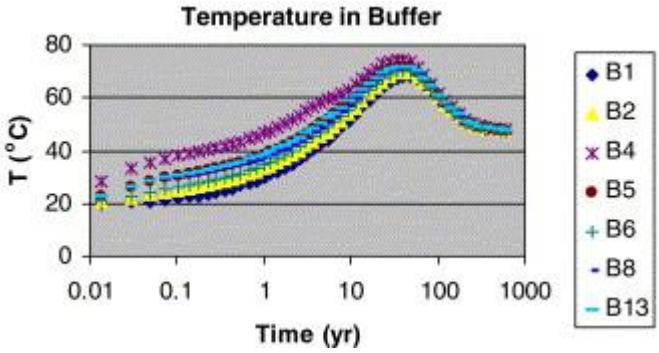

Fig. 9. Temperature profiles at various locations in the buffer (CNSC results).

The evolution of temperature at point B4 is summarized on Fig. 10. In this figure, the ISEB/ZAG curve relates to a purely TM calculation. As already observed from the previous DECOVALEX projects, there is a fair agreement between the temperature predictions, which are mostly dominated by heat conduction.

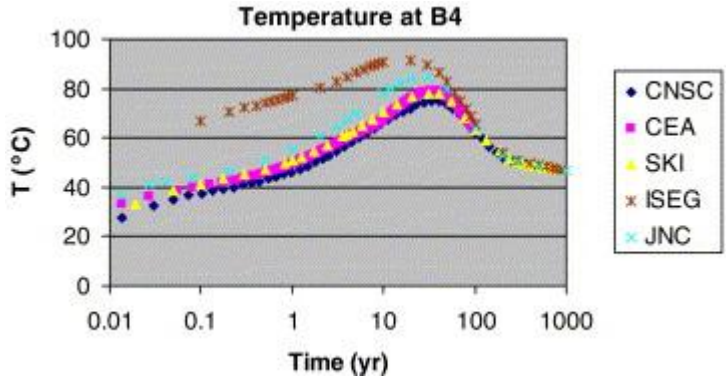

Fig. 10. Comparison of predicted temperature histories at point B4.

4.1.2. Evolution of saturation in the buffer and the time to full re-saturation

Contours of the liquid saturation at 1, 10 and 40 years are displayed in Fig. 11. The thermal gradient induced by the waste-released heat causes, first, a de-saturation close to the heater. After 1 year, a negative fluid pressure is obtained in the near-field rock, that is in the close vicinity of the buffer, the rock mass de-saturates. However, this effect remains minor, and at 10 years, the whole domain is fully saturated, except close to the canister. At point B4, the predictions of the degree of saturation of the buffer are compared (Fig. 12). The predicted time for full re-saturation varies between 7 years (CEA/IRSN) and 55 years (SKI/KTH). This discrepancy may be partly attributed to the fact that the water retention curves and the relative permeability dependence with saturation are different with different teams according to their engineering judgments.

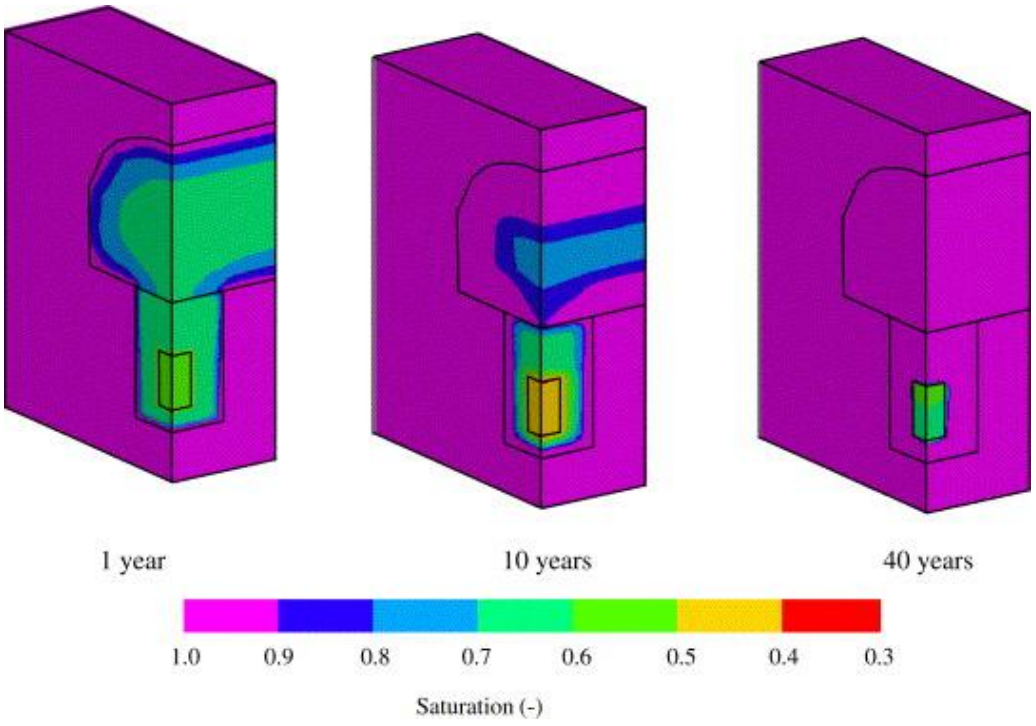

Fig. 11. Saturation contours at 1, 10 and 40 years (SKI/KTH results).

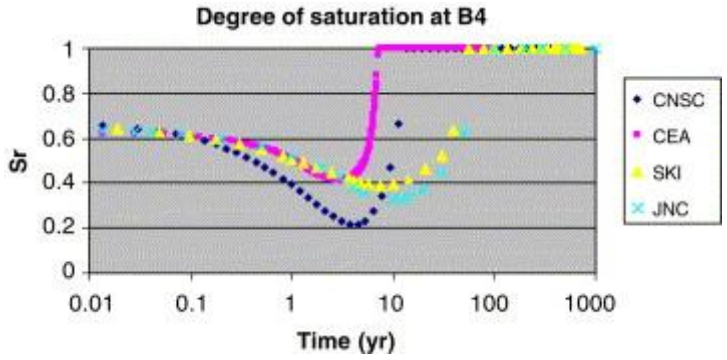

Fig. 12. Evolution of degree of saturation at point B4.

4.1.3. Evolution of stresses in the buffer

The development of stresses in the buffer is induced by different mechanisms:

• first, the bentonite swelling, as a result of the re-saturation,

• then, after full re-saturation, the fluid pore pressure increases from 0 MPa to hydrostatic pressure (10 MPa),

• in addition, thermal expansion may induce stresses due to the confinement of the bentonite by the rock.

The sum of these effects is illustrated on Fig. 13. A further study of the couplings effects will enable to quantify each of them.

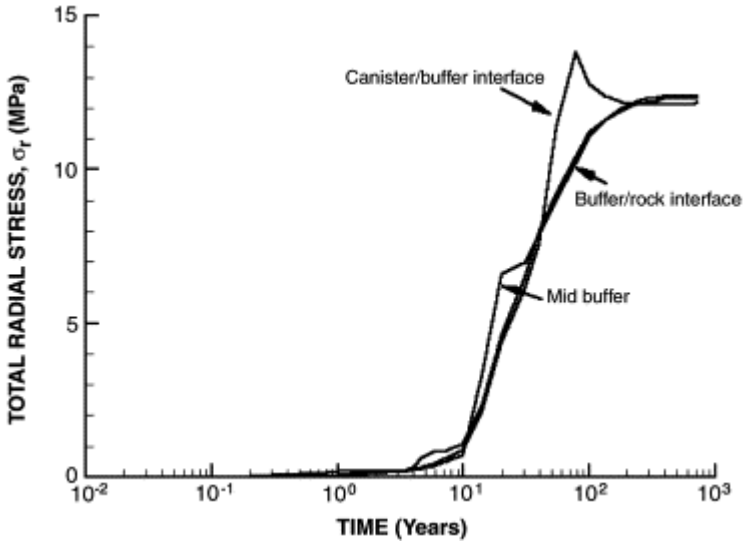

Fig. 13. Evolution of radial total stresses at three points in the buffer.

4.1.4. Evolution of stresses in the rock mass and possible rock failure

The safety factor for failure is defined as the ratio σ'_1/σ'_{1f} of the maximum principal effective stress σ'_{1f} and the maximum principal effective stress at failure is given by Eq. (3). A first possible failure may occur after excavation, at the floor of the gallery, where the maximum principal stress in tension can be higher than the tensile strength of the rock, due to the de-confinement of the rock. This possible failure was predicted by the CEA/IRSN, CNSC and SKI/KTH teams. Afterwards, during the heating phase, the highest possibility of failure would occur at around 100 years, according to SKI/KTH predictions, as can be seen from the safety factor contours plotted on Fig. 14. Again, the rock mass just below the drift and near the deposition hole is the most vulnerable for failure. After reaching a peak associated with the temperature paroxysm at about 40 years, the maximum compressive stress and also, the minimum compressive reduce, due to the combined effect of cooling and fluid pressure re-saturation. As a result, the effective minimum stress becomes close to tensile in the drift floor, basically in a direction normal to the drift floor surface. It causes a reduction of the rock strength, according to the Hoek–Brown criterion (cf. Eq. (3)), which, combined with a relatively high maximum compressive strength, could result in rock-mass failure.

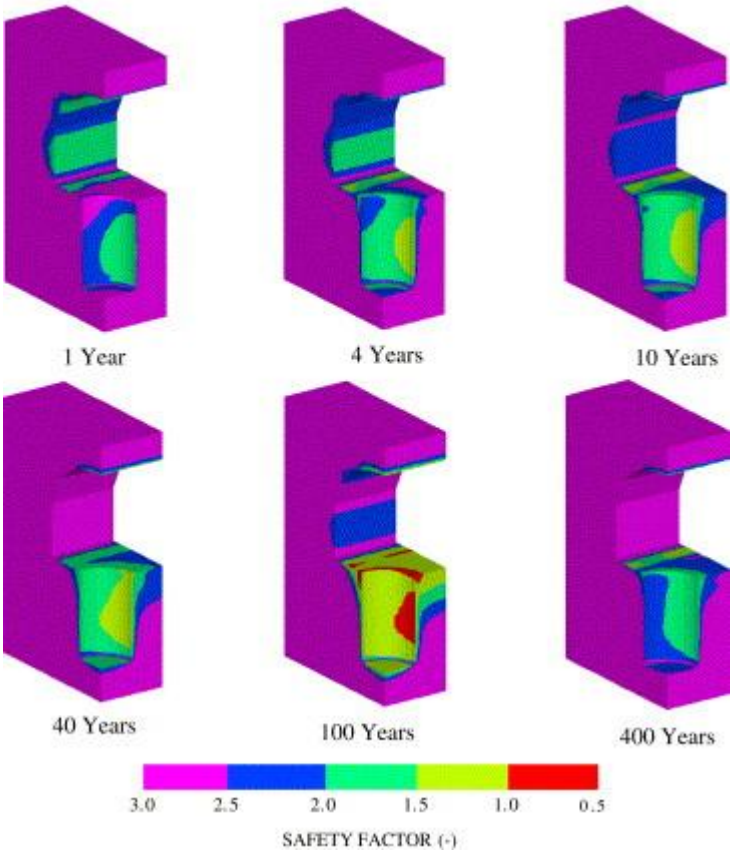

Fig. 14. Contours of safety factors in the near field rock.
A factor below 1 indicates failure (SKI/KTH results).

4.1.5. Permeability changes in rock

As may be expected, the excavation causes an increase of the rock-mass permeability at the floor of the drift, where tensile stresses were noticed (Fig. 15). Simultaneously, the rock surrounding the drift is overloaded by the vertical load, leading to an important reduction of the porosity and then permeability. With heating, additional compressive thermal stresses would develop, but their effect on the porosity would be counterbalanced by the pore pressure build-up associated with the re-saturation, leading to a more uniform permeability field at 100 years (Fig. 16).

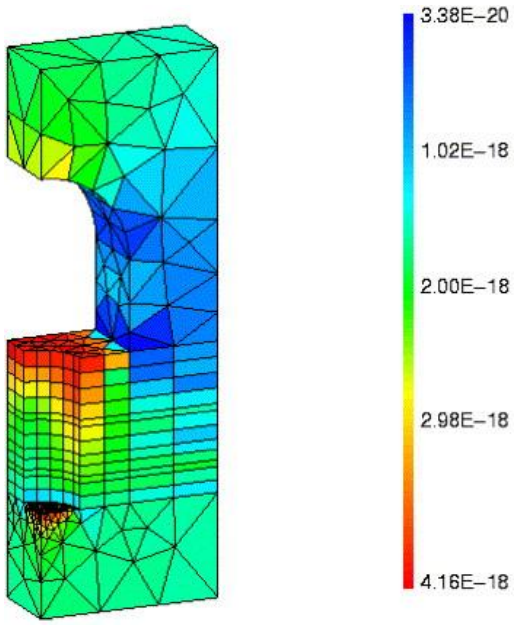

Fig. 15. Near-field rock mass permeability after excavation (CEA/IRSN results).

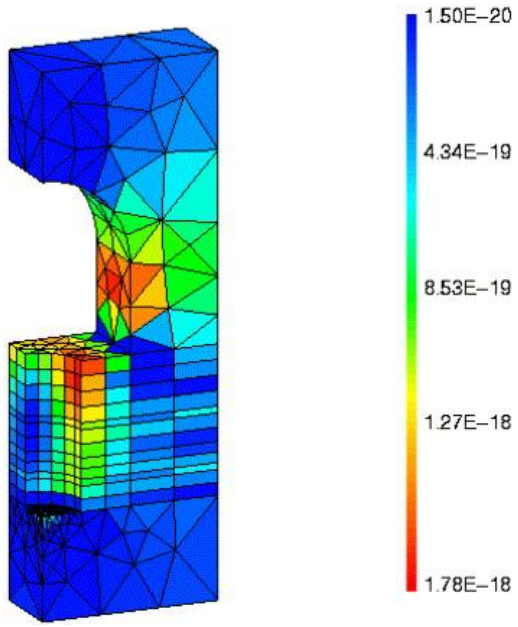

Fig. 16. Near-field rock mass permeability after 100 years (CEA/IRSN results).

4.2. Influence of the rock-mass permeability on the THM results

In addition to the base case (rock mass permeability K = 10^{-18} m^2), a low permeability (K = 10^{-19} m^2) and a high permeability (K = 10^{-17} m^2) have been considered. The results are discussed briefly here. A closer examination will be given in the next paragraph, when looking at the effect of the couplings.

Regarding the temperature predictions, the initial rock permeability has only a low influence, through the water content variations during the heat conduction.

Conversely, the rock permeability has a strong influence on the evolution of the saturation and the time for full re-saturation of the buffer, since it controls the water fed from the rock. For a low permeability, the buffer is not yet fully re-saturated after 100 years. Fig. 17 compares the evolution of the saturation degrees at three points in the buffer, for the base case permeability and for the low permeability. In the latter case, the delayed saturation implies that the swelling stresses in the buffer also developed slowly, which has a significant impact on the mechanical stability of the surrounding rock mass. As a consequence, the radial stresses in the buffer are still close to zero at 100 years, and the buffer provides no significant support forces on the walls of the drift and deposition hole. This leads to the development of a zone of extensive failure in the floor of the drift.

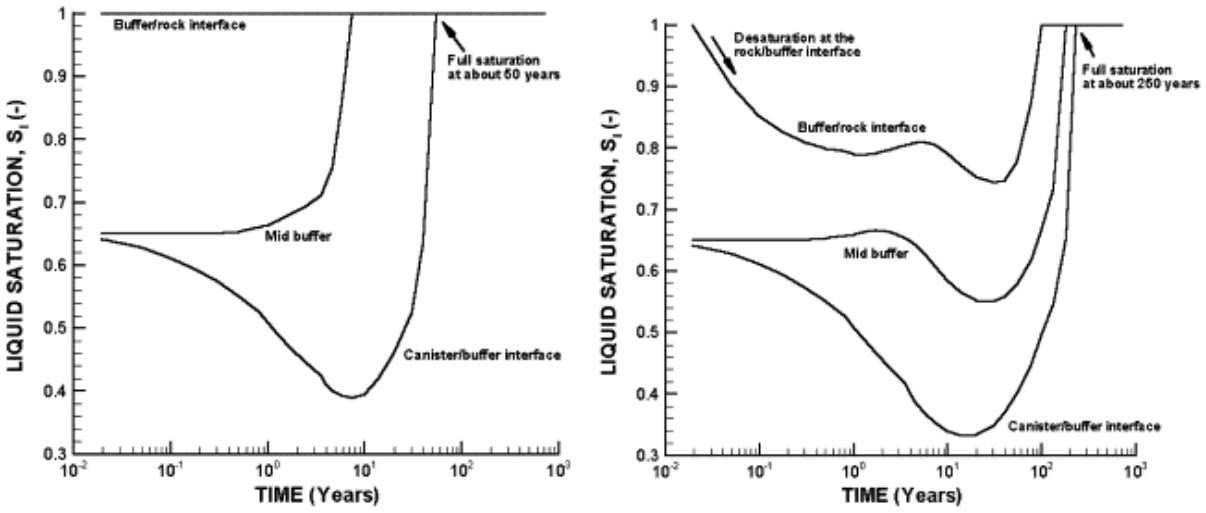

Fig. 17. Evolution of the saturation at 3 points in the buffer.
Left: base case; right: low permeability (SKI/KTH results).

5. Evaluation of effects of different coupling combinations

In this section, the importance of the couplings on the performance measures is evaluated by comparing the THM calculations to the partially uncoupled combinations: TH, TM, and HM. In addition, the influence of the initial rock-mass permeability was also investigated through scoping calculations.

5.1. Temperature evolution in the buffer and maximum temperature

A very limited effect, of a few degrees, was found on the temperatures, with the maximum difference arising close to the canister (point B4) and for the low rock permeability case. It is due to the variation of the thermal conductivity induced by the changes in saturation, as already outlined in Section 4.2. This variation is considered only when the coupling from H to T is included, which is the case in a TH and THM analysis. An illustration is given in Fig. 18, for points B4 and B6, in the base case of the rock permeability. From these results, the evolution of saturation in the buffer and the time for full re-saturation indicate that, in the present analysis, the temperature distribution can be reasonably predicted by a single uncoupled thermal analysis of heat conduction.

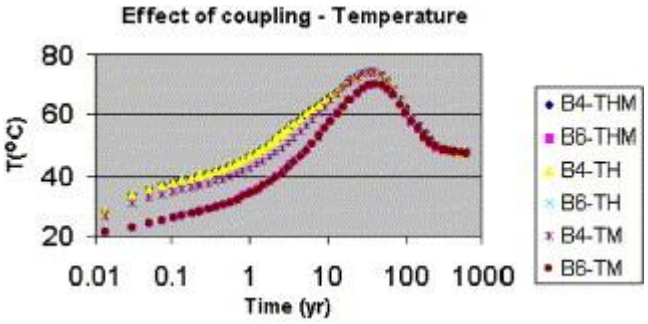

Fig. 18. Temperature at points B4 and B6 for different couplings—Base case (CNSC results).

5.2. Evolution of saturation in the buffer and the time for full re-saturation

Unlike with temperature, the situation is completely different for the saturation, or, equivalently, the pore pressure. In fact, for medium rock-mass permeability (base case) or high permeability, the TH and THM analyses lead to similar evolutions of the liquid saturation in the buffer, close to the canister. In these cases, the saturation degree is controlled mainly by the vapor diffusion associated to the thermal gradient, while the rock supplies water sufficiently rapidly. For the low-rock permeability, a correct prediction of the buffer saturation and pore pressure requires a full THM analysis, as demonstrated in Fig. 19 and Fig. 20. At early times, the rock does not supply enough water to the buffer, leading to a drop in pore pressures. At the interface between the buffer and rock (point B6), rebuilding of the hydrostatic pressure starts at about 30 years for the THM case, and at about 60 years for the HM case, while it is still unsaturated after 100 years in the TH case (Fig. 20).

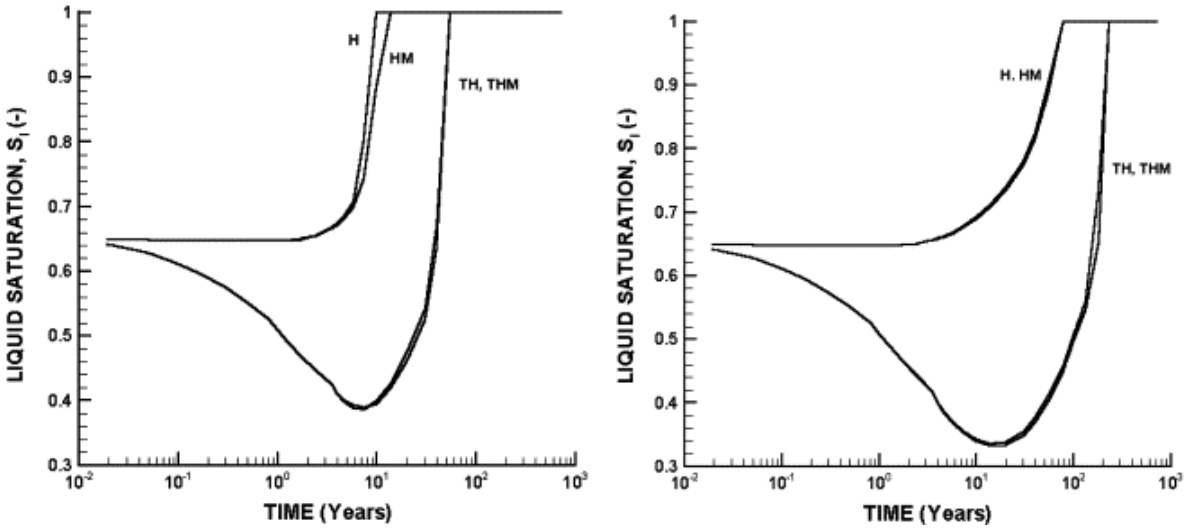

Fig. 19. Saturation at point B4 for different couplings—Left: base case; right: low permeability (SKI/KTH results).

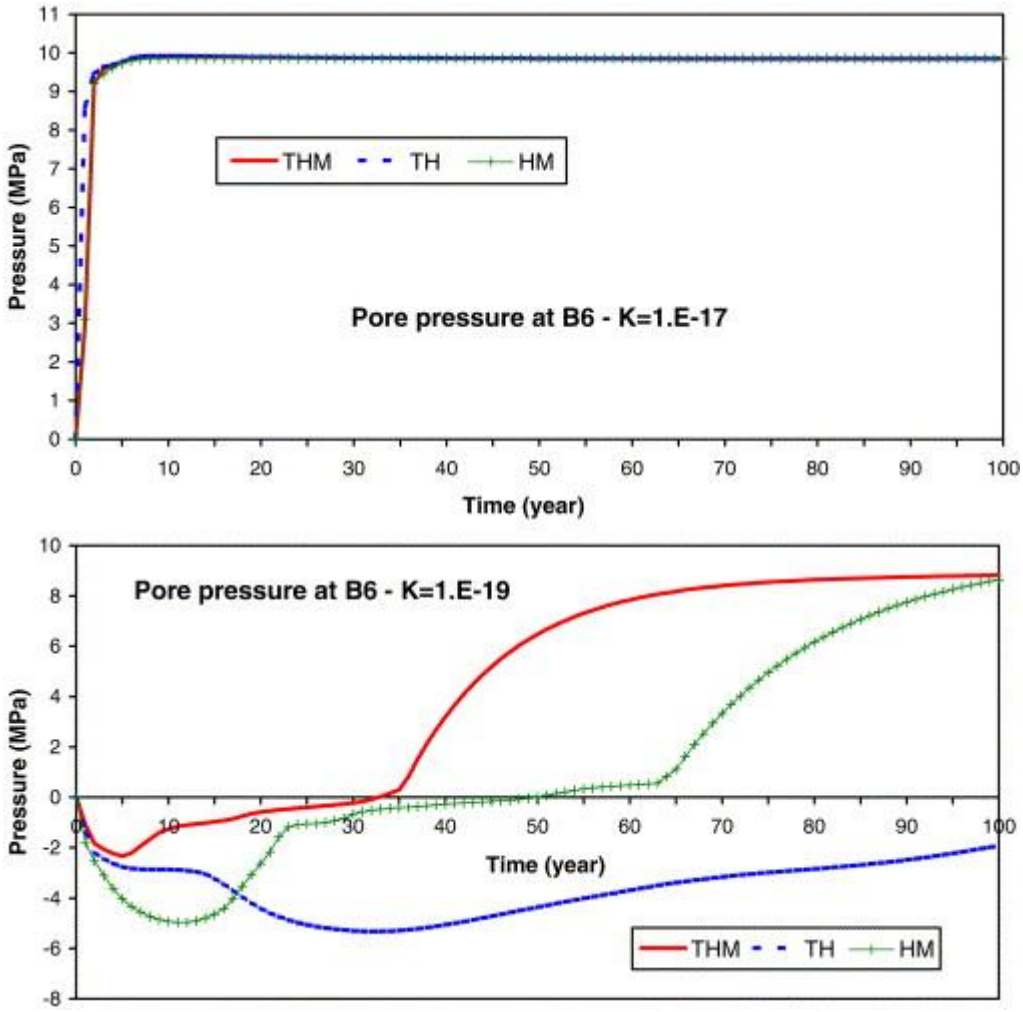

Fig. 20. Pore pressures at point B6 for different couplings–Top: high permeability, bottom: low permeability (CEA/IRSN results).

5.3. Evolution of stresses in the buffer

As might be expected, couplings have a strong effect on the total stresses, on the one hand, because of the thermally induced stresses (of order of magnitude of 0.1 Mpa), and on the other hand, because of the swelling pressure of the buffer and the hydrostatic pressure contributions. (This latter effect is of the order of magnitude of 10 Mpa and is predominant.) This is clearly visible in Fig. 21 that shows the evolution of the maximum compressive stress at the interface between the buffer and the canister.

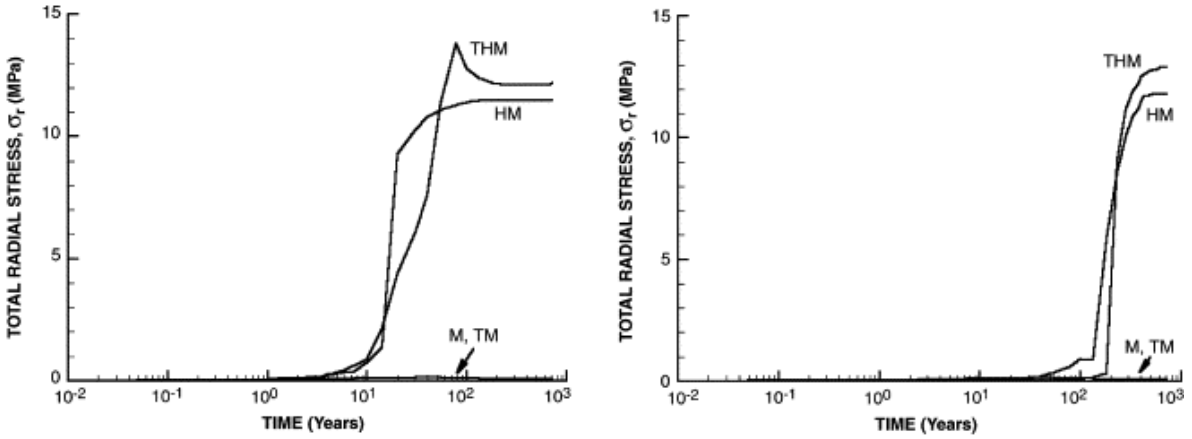

Fig. 21. Maximum compressive stress at point B4 for different couplings—Left: base case; right: low permeability (SKI/KTH results).

The same observations can be made for all three values of permeability, when looking for example at the point B6 (Fig. 22). In conclusion, HM coupling is extremely important for the correct prediction of the stresses in the buffer.

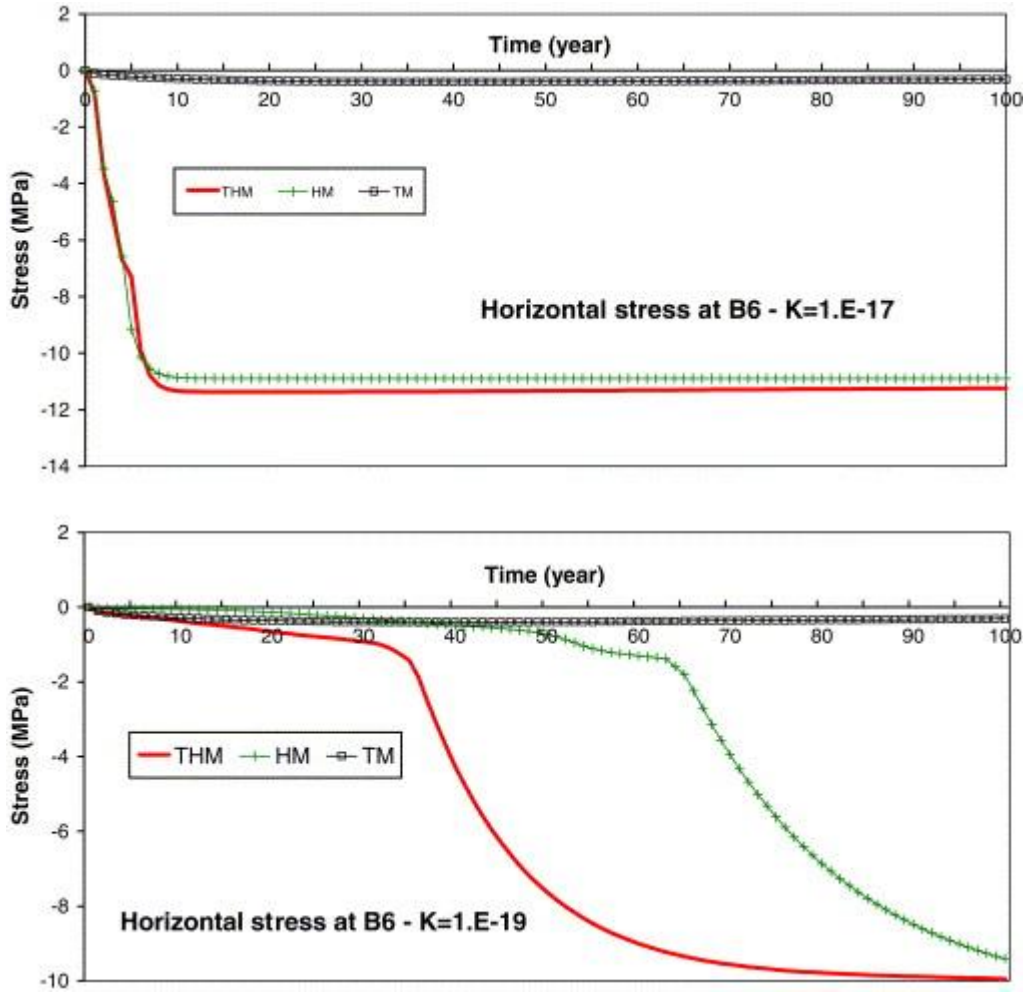

Fig. 22. Radial stress at point B6 for different couplings—Top: high permeability; bottom: low permeability (CEA/IRSN results).

5.4. Evolution of stresses in the rock mass and possible rock failure

Failure is conditioned to the effective stress state, according to Eq. (3). As already mentioned, possible failure may occur either after excavation or after the thermal paroxysm. The influence of the couplings on the safety factor is presented after excavation (Fig. 23) and after 100 years of heating (Fig. 24). It appears that it is necessary to account for both TM and HM couplings to predict the mechanical integrity of the rock mass. At 100 years, in the HM analysis, failure is prevented because the swelling of the bentonite provides a support load to the rock mass. This also explains why the TM analysis indicates most failure.

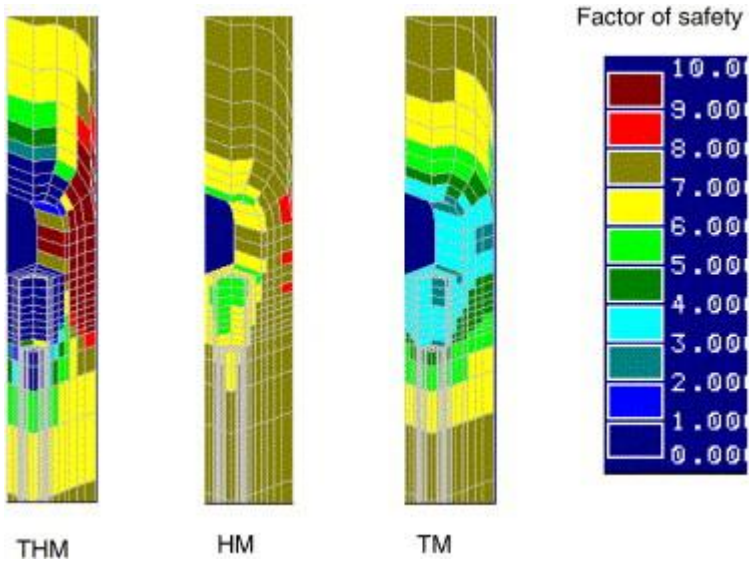

Fig. 23. Effect of couplings on rock-mass stability after excavation base case (CNSC results).

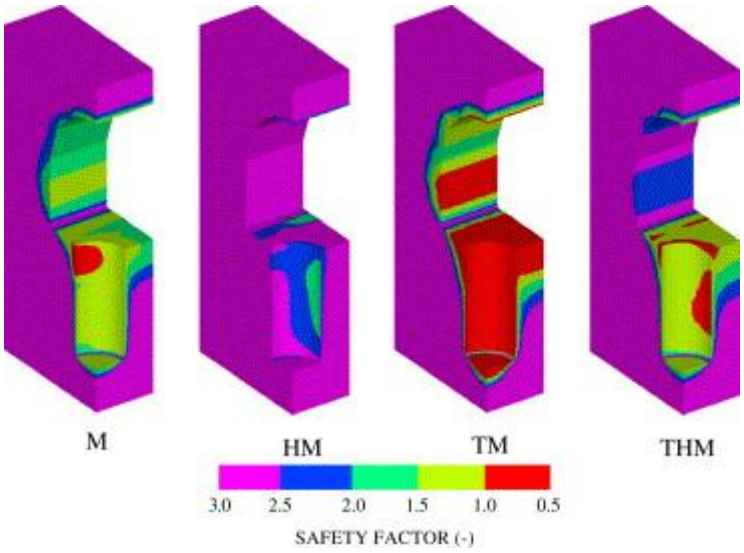

Fig. 24. Effect of couplings on rock-mass stability after 100 years of heating base case (SKI/KTH results).

5.5. Permeability changes in rock

As outlined in Section 2.3, two different laws of variation of permeability have been proposed. Therefore, the effects of the couplings on the permeability changes depend highly on the chosen law. For example, in the case of a stress-induced permeability change, only the HM and THM analyses are concerned, and they lead to significant differences: the HM predictions are mostly affected by the excavation phasis leading to an increase of the permeability, while the THM predictions show an inverse tendency due to the additional effect of the thermal stresses (see Fig. 25).

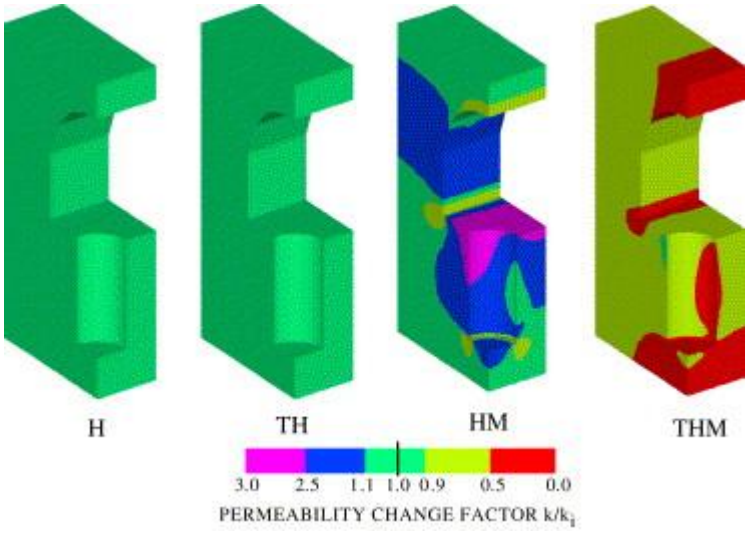

Fig. 25. Effect of couplings on rock-mass permeability after 40 years of heating base case (SKI/KTH results).

In the case of a porosity-induced permeability change, variations of porosity are possible even in TH analysis, due to allowance for thermal strains of the solid grains. In CNSC results, the thermal effects are responsible for a 60% increase of the permeability at excavation. Afterwards, they interplay with the pore pressure effect. (see Fig. 26).

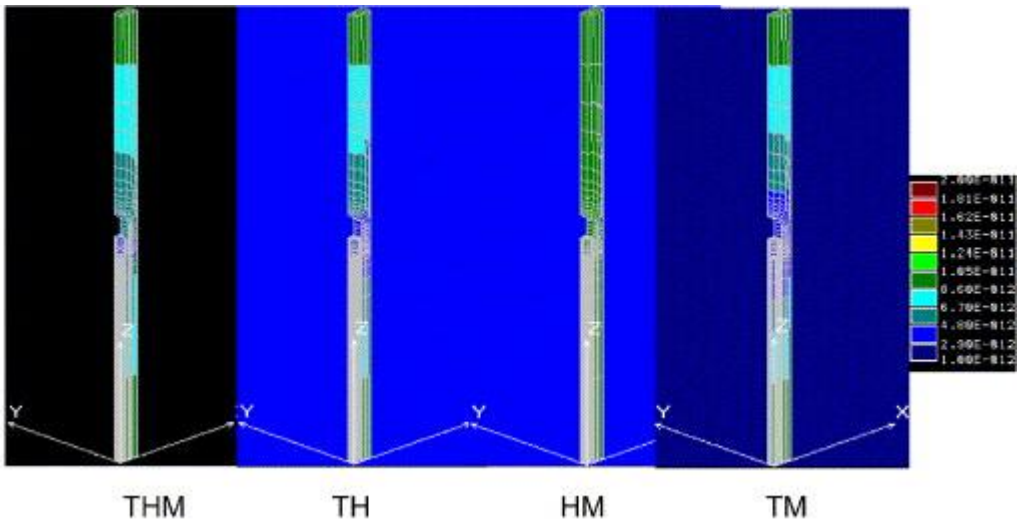

Fig. 26. Effect of couplings on rock-mass permeability after 40 years of heating high permeability (CNSC results).

In both cases, again the THM analysis is required for a most realistic prediction.

6. Concluding remarks

In this paper, the impact of coupled THM processes on the performance of an hypothetic repository, located in an homogeneous rock mass, has been investigated. This hypothetical repository possesses composite features since it is based on a Japanese design, with a Japanese bentonite used as buffer material and the heat output characteristics of Japanese spent fuel. However, the permeability and strength characteristics of the rock mass are based on typical properties of granites of the Canadian shield.

The evaluation of the effect of the couplings was achieved by first performing a fully coupled THM analysis, followed by partially uncoupled ones: TH, TM, HM. Moreover, the effect of the initial rock-mass permeability, which controls the time to re-saturation of the buffer, has been appraised. Some basic performance measures have been predefined for comparison:

• evolution of the temperature in the buffer, and in particular the maximum temperature,

• evolution of the moisture content in the buffer, and in particular the time for full saturation,

• evolution of the stresses in the buffer and its maximum,

• possibility of a rock-mass failure,

• maximum change of permeability in the rock mass.

The results presented in the paper can be synthesized as follows:
• for the temperature evaluation, there is no significant effect of H and M couplings, and the conduction process dominates,

• re-saturation of the buffer is affected by T coupling but not significantly by M coupling

• stress evolution in the buffer is strongly affected by H coupling, the pore pressure build-up representing the major part of the total stress, and is only slightly affected by T coupling,

• possible rock-mass failure is strongly affected by both T and H couplings

These major findings are summarized in Table 4.

Table 4. Effects of THM couplings on near-field repository response

Indicator	**THM**	**TH**	**TM**	**HM**
Temperature	Low	Low	Low	—
Resaturation	Medium/High	Medium	—	Low
Swelling stress	High	—	Low	High
Rock failure	High	—	Low	High
Permeability change	Medium/High	Medium	Medium	Low

In addition to this table, the crucial role of the initial rock-mass permeability has been highlighted. For confident building and demonstration purposes, a fully coupled approach is necessary to interpret monitoring data that would be collected during the first decades after the repository closure.

Of course, the conclusions of this paper are limited to the case under consideration, that is the case of a homogeneous rock mass. The presence of fractures in the rock mass and its consequences are the subject of a companion paper [4].

Acknowledgments

The authors sincerely thank the funding organizations, ANDRA, BGR, CNSC, IRSN, JNC and SKI for their financial support and all participants of DECOVALEX III for very useful feedback on the work presented in this paper.

References

[1] Jing L, Tsang C-F, Mayor J-C, Stephanson O, Kautsky F, editors. DECOVALEX III—Mathematical models of coupled thermal-hydro-mechanical processes for nuclear waste repositories—executive summary. Technical report 2005:19, Swedish Nuclear Power Inspectorate.

[2] Jing L, Stephansson O, Börgesson L, Chijimatsu M, Kautsky F, Tsang C-F. DECOVALEX II, Technical Report–Task 2C. SKI Report 99:23, 1999.

[3] Chijimatsu M, Nguyen TS, Jing L, De Jonge J, Kohlmeier M, Millard A, Rejeb A, Rutqvist J, Souley M, Sugita Y. Numerical study of the THM effects on the near-field safety of a hypothetical nuclear waste repository—BMT1 of the DECOVALEX III project. Part 1: conceptualization and charactertization of the problems and summary of results. Int J Rock Mech Min Sci 2005; (this issue).

[4] Rutqvist J, Chijimatsu M, Jing L, Millard A, Nguyen TS, Rejeb A, Sugita YA, Tsang C-F. Numerical study of THM effects on the near-field safety of a hypothetical nuclear waste repository–BMT1 of the DECOVALEX III project. Part 3: effects of THM coupling in sparsely fractured rocks. Int J Rock Mech Min Sci (this issue), 2005.

[5] Japan Nuclear Cycle Development Institute. Second progress report on research and development for the geological disposal of HLW in Japan, H12: project to establish the scientific and technical basis for HLW disposal in Japan. Project overview report, JNC TN1410 2000-001, 2000.

[6] M. Chijimatsu, T. Fujita, Y. Sugita, K. Amemiya and A. Kobayashi, Field experiment, results and THM behavior in the Kamaishi mine experiment, Int J Rock Mech Min Sci 38 (2001) (1), pp. 67–78.

[7] J. Rutqvist, J. Börgesson, M. Chijimatsu, A. Kobayashi, L. Jing, T.S. Nguyen, J. Noorishad and C-F. Tsang, Thermohydromechanics of partially saturated geological media:

governing equations and formulation of four finite element models, Int J Rock Mech Min Sci 38 (2001) (1), pp. 105–128.

[8] J. Rutqvist, J. Börgesson, M. Chijimatsu, T.S. Nguyen, L. Jing, J. Noorishad and C-F. Tsang, Coupled thermo-hydro-mechanical analysis of a heater test in fractured rock and bentonite at Kamaishi mine—comparison of field results to predictions of four finite element codes, Int J Rock Mech Min Sci 38 (2001) (1), pp. 129–142.

[9] Nguyen TS, Jing L, editors. DECOVALEX III/BENCHPAR Projects report of BMT1B/WP2—implications of T-H-M coupling on the near-field safety of a nuclear waste repository in a homogeneous rock-mass. Technical report 2005:25, Swedish Nuclear Power Inspectorate.

[10] E. Hoek and E.T. Brown, Practical estimates of rock mass strength, Int J Rock Mech Min Sci 34 (1997), pp. 1165–1186.